International Journal on Advanced Science Engineering Information Technology

Vol.12 (2022) No. 2
ISSN: 2088-5334

Mathematical Model of Radio Frequency Assisted Heat Pump Drying of Ganoderma Lucidum (*Ganoderma Boninense*)

Nguyen Hay [a], Le Anh Duc [a,*], Pham Van Kien [b]

[a] *Nong Lam University, Ho Chi Minh City, Vietnam*
[b] *Faculty of Automotive Engineering, School of Engineering and Technology, Van Lang University, Ho Chi Minh City, Vietnam*
*Corresponding author: *leanhduc@hcmuaf.edu.vn*

Abstract—**This study proposed a mathematical model which was used to predict the temperature and moisture content of Ganoderma lucidum (*Ganoderma boninense*) during the radio frequency (RF) assisted heat pump (HP) drying process. The simultaneous heat and mass transfer equations were established based on the physical and flat plate models for drying Ganoderma lucidum and the specific assumptions for the proposed problem. The finite difference method was used to solve the proposed heat transfer and moisture transfer problem, in which, *pdepe* function was adjusted and complemented with Matlab software. The temperature and moisture content of the material in the drying process was predicted. The effect of the output RF power on the temperature and moisture content of the material was evaluated. The drying process's input parameters were drying air temperature of 40ºC, air velocity of 1.2 m/s, and an output RF power of 1.95 kW, 0.65 and 0 kW. The results showed that when the output RF power increases, the heating rate increases, and the drying time is shortened significantly. The drying material temperature reaches the drying air temperature in 20 minutes, 30 minutes, and 220 minutes and the drying time is 465, 555, and 700 minutes, corresponding to output RF power of 1.95 kW, 0.65 and 0 kW. The predicted temperature and moisture content of the material were compared with experimental drying data, and a considerably good agreement was found.**

Keywords—**Radio frequency; heat pump; Ganoderma Lucidum; finite difference; mathematical modeling.**

Manuscript received 5 Aug. 2019; revised 14 Dec. 2021; accepted 20 Jan. 2022. Date of publication 30 Apr. 2022.

I. INTRODUCTION

Ganoderma lucidum is one kind of medicinal product. The moisture content of fresh Ganoderma lucidum is 3 (d.b) and it is usually preserved in dry form. Ganoderma lucidum has some properties such as woody and spongy structure, low heat transfer coefficient, and low moisture exhausting capacity. Ganoderma lucidum contains some bioactive ingredients, and Polysaccharides is a crucial ingredient, which have effects of effective treatment for tumor, inflammation, cancer, and HIV [1]. However, Polysaccharides as well as other bioactive ingredients in Ganoderma lucidum are thermo-sensitive substances and will be degraded by the high drying temperature. There were previous studies of experimental drying Ganoderma lucidum to determine a suitable drying method with the optimum input drying parameters to obtain a high Polysaccharide content of Ganoderma lucidum after drying [2]–[4]. The results showed that the suitable drying method to retain Polysaccharide's high content in Ganoderma lucidum was drying at low temperature in the range of 45 - 65°C. When the drying temperature exceeded 65°C, Polysaccharides' content tended to degrade because of thermal degradation. When the drying temperature was lower than 45°C, the drying time would increase and Ganoderma lucidum would be exposed to hot drying air longer. This made Polysaccharides content in Ganoderma lucidum decrease.

There were some studies of drying techniques using RF. Nguyen Hay et al. studied the RF assisted HP dryer's effect in drying Ganoderma lucidum [5]. The results showed that in RF assisted HP drying process, the drying time decreased significantly, and the Ganoderma lucidum after drying still retained higher Polysaccharide content. Jumah theoretically analyzed the process of RF assisted fluidised bed drying of particulates, and the results indicated that the moisture distribution inside the corn influenced on the drying kinetics significantly [6]. Ptasznik et al. studied the RF assisted convective drying of shrinkable and hygroscopic materials, in which a semi-empirical model for the drying process was developed. The simulation results indicated that the heat generation inside drying material significantly affected the temperature of dried product and the drying kinetics [7].

Marshall and Metaxas studied the RF-assisted HP drying of particulate materials and the results showed that the combined system's dryer and HP performance could be improved [8].

The mathematical models of heat transfer in the drying process using RF for food and agricultural products were studied [9]–[12]. In the studies, the heat transfer equation, which took into account the convective heat exchange, the heat conduction, and the heat generated within the material by RF power dissipation, was established.

In drying using the RF process, RF's volumetric heating mechanism significantly increases the heating rate and drying rate. However, in the RF heating process, the material's temperature is relatively high and tends to increase over the temperature of drying air from 7 to 35°C [13],[14]. Thus, in order that the temperature of Ganoderma lucidum achieves the suitable value required, the temperature of drying air and the RF power has to be chosen carefully. The experiments on RF heating rate and RF power absorption showed that the temperature of drying material increases from 47 to 65°C when the RF power was chosen in the range of 0.65 - 1.95 kW and the drying air temperature was chosen in the range of 40 - 50°C. That not only shortens the drying time but also retains the high bioactive ingredients content in Ganoderma lucidum.

This study was conducted basing on the objectives as: (1) to develop a mathematical model of RF assisted heat pump drying process; (2) to investigate the effects of the output RF power on the temperature and moisture content of the drying material.

II. Material and Method

A. Material

The red Ganoderma lucidum (*Ganoderma Boninense*) was the drying material used in the drying experiments. The Ganoderma lucidum samples had a moisture content of 3 (d.b), an average diameter of 0.15 m and an average thickness of 0.015 m. A moisture analyzer (DBS 60-3 model) was used to determine the material samples' initial moisture content.

B. Mathematical Model of Radio Frequency Assisted Heat Pump Drying of Ganoderma Lucidum

Figure 1 gave the model for RF-assisted HP drying of Ganoderma lucidum. The Ganoderma lucidum samples were placed on a plastic mesh grid drying trays which were placed between two RF electrodes in a drying chamber. The RF electrodes were separated with 150 mm by Teflon plastic bars. Consequently, the heat exchange area with drying air on the lower side of the material was less than that on the upper side. However, the heat exchange area reduction was tiny compared to the material samples' overall surface area. Thus, the heat exchange processes at two surfaces of the material samples were assumed to be the same in the present analysis.

The model for RF-assisted HP drying of Ganoderma lucidum as in Fig. 1, the physical model for drying Ganoderma lucidum, was described in Fig. 2. In the drying process, the drying air was blown through the heat pump system and into the drying chamber for the drying process. The drying process was conducted under the combination of the drying air and the RF generator's RF.

In addition to the assumptions given above, the drying process's mathematical model assumed that the heat and mass transfer processes within the material are in one dimension in the x-direction as in Fig. 3.

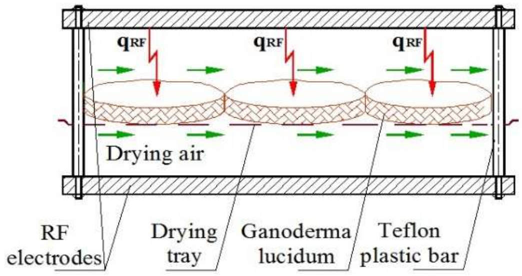

Fig. 1 The model for RF assisted HP drying of Ganoderma lucidum

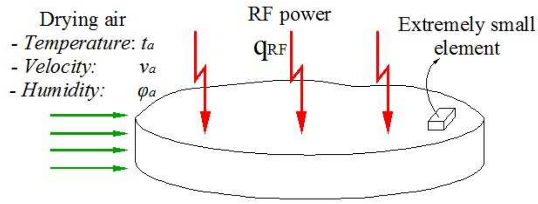

Fig. 2 Physical model for drying of Ganoderma lucidum

Fig. 3 Flat plate model for drying Ganoderma lucidum

The mathematical model was developed by the assumptions [15] as follows: the heat transfers by radiation are not considered, and heat transfer only includes conduction and convection; initial temperature and moisture distribution in the material are both uniforms; no chemical reaction nor moisture generation takes place in the material; deformations are small and negligible; thermo-physical properties of the material depend on both temperature and moisture content.

Basing on the physical model for drying Ganoderma lucidum, flat plate model for drying Ganoderma lucidum and the assumptions above, the 1-D heat and mass transfer equations was written as below:

The heat transfer equation:

$$\underbrace{\rho C_p \frac{\partial t}{\partial \tau}}_{1^{st}} = \underbrace{\lambda \frac{\partial^2 t}{\partial x^2}}_{2^{nd}} + \underbrace{r\rho_k \frac{\partial M}{\partial \tau}}_{3^{rd}} + \underbrace{q_{\mathrm{RF}}}_{4^{th}} \tag{1}$$

The mass transfer equation:

$$\frac{\partial M}{\partial \tau} = D\frac{\partial^2 M}{\partial x^2} \tag{2}$$

In the heat transfer equation, the first term is internal energy change within the material, and the second term is heat transfer by conduction within the material, the third term is the heat required for vaporization of moisture within the material, and the fourth term is heat generated within the material by RF power dissipation.

The corresponding initial conditions are given as:

At $\tau = 0$:

$$t(x,0) = t_0; M(x,0) = M_0 \tag{3}$$

The heat and mass transfer boundary conditions ($\tau > 0$) are given as:

At x = 0:

$$\left.\frac{\partial t}{\partial x}\right|_{x=0} = 0; \left.\frac{\partial M}{\partial x}\right|_{x=0} = 0 \quad (4)$$

At x = δ/2:

$$-\lambda\left.\frac{\partial t}{\partial x}\right|_{x\equiv x_s} = \alpha(t_a - t)\Big|_{x\equiv x_s} - r\rho_k\beta_M(M - M_e)\Big|_{x\equiv x_s} \quad (5)$$

$$-D\left.\frac{\partial M}{\partial x}\right|_{x\equiv x_s} = \beta_M(M - M_e)|_{x\equiv x_s} \quad (6)$$

C. The Method of Solving the Heat and Mass Transfer Equations

The finite difference method was used to solve numerically the heat and mass transfer equations that were proposed in the section "B" [16].

The general equation form of a partial differential equation (PDEs) w as given below.

$$A(x,y)\frac{\partial^2 u}{\partial x^2} + B(x,y)\frac{\partial^2 u}{\partial x \partial y} + C(x,y)\frac{\partial^2 u}{\partial y^2} = f\left(x, y, u, \frac{\partial u}{\partial x}, \frac{\partial u}{\partial y}\right) \quad (7)$$

In which variable x, y are in range: $x_0 < x < x_f$; $y_0 < y < y_f$ and they must satisfy the boundary conditions that are boundary condition functions along the boundary of x and y. The partial difference problem contains the types of boundary condition as Dirichlet: $u = b_0$, Neumann $\left(\frac{\partial u}{\partial x}, \frac{\partial u}{\partial y}\right) = b_0$ and complex of Dirichlet and Neumann.

According to the condition as: $B^2 - 4AC$, there are three types of problem:

$$\begin{cases} Elip\ PDE\ if: B^2 - 4AC < 0 \\ Parabol\ PDE\ if: B^2 - 4AC = 0 \\ Hyperbol\ PDE\ if: B^2 - 4AC > 0 \end{cases} \quad (8)$$

In the present study, to solve the heat and mass transfer equations, the finite difference solution procedure with the space domain as half of Ganoderma lucidum thickness (δ) using Matlab 2016a. The space domain x [0; x_f] is divided into N elements with thickness of $\Delta x = x_f/N$. The time-domain τ is divided into K elements with a time value of $\Delta\tau = \tau_f/K$, where τ_f is the total time. Finding the function t(x,τ) and M(x,τ) becomes finding values at nodes t_i^j, M_i^j as i = 1,2,…,N; j = 1,2,…,K [17].

The partial differential equations of the function u(x,τ) is rewritten by first and second-order differential forms as:

$$\begin{cases} \left.\frac{\partial u(x,t)}{\partial t}\right|_{x_i, \tau_k} \approx \frac{u_i^{j+1} - u_i^j}{\Delta\tau} \\ \left.\frac{\partial^2 u(x,t)}{\partial x^2}\right|_{x_i, \tau_k} \approx \frac{u_{i+1}^j - 2u_i^j + u_{i-1}^j}{(\Delta x)^2} \end{cases} \quad (9)$$

In which, i = 1,2,…,N-1; j = 1,2,…,K

The problem of Neumann boudary condition has the forms as:

$$\begin{matrix} \left.\frac{\partial u}{\partial x}\right|_{x=0} = b_0 \\ \left.\frac{\partial u}{\partial x}\right|_{x\equiv x_s} = b_1 \end{matrix}, thus \begin{matrix} \frac{u_1^j - u_0^j}{\Delta x} = b_0(j) \\ \frac{u - u_{N-1}^j}{\Delta x} = b_1(j) \end{matrix} \quad (10)$$

Equation (9) is an equation of t and M in the heat and mass transfer problem.

If $u = \begin{bmatrix} t \\ M \end{bmatrix}$, a partial differential equation with the variable of vector u is obtained from a partial differential equation.

In the present study, the heat and mass transfer equations are rewritten by partial difference form as:

$$\begin{cases} \frac{t_i^{j+1} - t_i^j}{\Delta\tau} = \frac{1}{\rho^j . C_p^j}\lambda^j \frac{t_{i+1}^j - 2t_i^j + t_{i-1}^j}{(\Delta x)^2} + \cdots \\ \cdots + \frac{1}{\rho^j . C_p^j} r . \rho_k \frac{M_i^{j+1} - M_i^j}{\Delta\tau} + \frac{1}{\rho^j . C_p^j} q_{\mathrm{RF}}^j \\ \frac{M_i^{j+1} - M_i^j}{\Delta\tau} = D\frac{M_{i+1}^j - 2M_i^j + M_{i-1}^j}{(\Delta x)^2} \end{cases} \quad (11)$$

The equation of heat and mass transfer boundary condition are rewritten by partial difference form as:

$$-\lambda^j \frac{t_{i+1}^j - t_i^j}{\Delta x} = \alpha . \left(t_a - t_i^j\right) - r . \rho_k . \beta_M . \left(M_i^j - M_e^j\right) \quad (12)$$

$$-D\frac{M_{i+1}^j - M_i^j}{\Delta x} = \beta_M . \left(M_i^j - M_e^j\right) \quad (13)$$

Within the scope of the proposed heat transfer and moisture transfer problem, the heat transfer program is developed on Matlab software to solve the problem. In the heat-transfer function, the PDEs problem is solved by *pdepe* function that was adjusted and complemented.

Thermo-physical properties and the drying conditions used to conduct the simulation and experimental drying were given in Table 1.

To evaluate the effect of the output RF power in the drying method of RF-assisted HP, the following values of output RF power were used: P_{RF} = 0, 0.65 and 1.95 kW. At P_{RF} = 0 kW, the drying mode corresponded to heat pump only drying mode.

TABLE I

DRYING CONDITIONS AND DRYING MATERIAL PROPERTIES

The thickness of samples, 2δ (m)	0.015
λ (W/m.°C)	$0.26+0.022\times M^3-0.141\times M^2+0.314\times M$
ρ (kg/m³) [18]	$599.9+57.287\times M+16.351\times M^2$
C_p, (J/kg.°C) [18]	$3017.5 + 541.616 \times \mathrm{Ln}M$
r (J/kg) [18]	$616.561 \times M_e^{(-0.938+0.008.t)} + 3.796 \times \ldots \ldots \times t^{(1.428-0.703.M_e)} + 2995.509 \times M_e - \ldots \ldots -2.055 \times t$
M_e (d.b) [19]	$[0.403 - 0.069.\ln[-(T + 24.05)].\ln(R_H)]].10^{-2}$
M_i (d.b)	3
t_i (°C)	27
t_a (°C)	50
R_H	18%
α (W/m².°C)	12.323
β_M (m/s)	0.012

D. Experimental Method

The drying process was conducted under controlled temperatures and RF power conditions. The model for RF-assisted HP drying of Ganoderma lucidum was given in Fig. 1. The RF operator operated with a frequency of 27 MHz. The input parameters of RF-assisted HP drying experiments of

Ganoderma Lucidum were drying air temperature of 40ºC, drying air velocity of 1.2 m/s, and RF power of 0, 0.65, and 1.95 kW. In which, at RF power of 0 kW, only HP drying method was used.

An electronic scale digital balance (DS–2002-N with a maximum measurement value of 2000 ± 0.001 g) was used to measure the Ganoderma lucidum sample weight regularly every 10 minutes during the drying process. The measurements were completed in triplicates when the drying material's moisture content reached 0.15 (d.b).

The temperature of Ganoderma lucidum was measured by two temperature sensors (AYN-MF59-104F-3950FB-1000) with measurement ranges of -60°C – 300°C ± 0.01ºC. The temperature sensors were connected to a computer software via an integrated circuit that could determine the temperature value versus drying time. The two small sensor heads of 1.05 mm were fixed inside a Ganoderma lucidum sample. The temperature value of Ganoderma lucidum was recorded by computer software every 10 minutes.

E. The Method Of Evaluating The Theoretical Mathematical Model

The theoretical mathematical model was evaluated by the difference between the heat and mass equations solving results and experimental drying data, in which the Root mean square error (RMSE) and Mean absolute error (MAE) were used and defined in Eq. (14) and Eq. (15):

$$\mathrm{RMSE} = \left[\frac{1}{N}\sum_{I=1}^{N}\left(V_{Exp} - V_{Pre}\right)\right]^{0.5} \tag{14}$$

$$\mathrm{MAE} = \frac{1}{N}\sum_{I=1}^{N}\left(\frac{|V_{Exp}-V_{Pre}|}{V_{Pre}}\right) \tag{15}$$

III. Results and Discussion

A. Effect of Output RF Power on the Temperature of Drying Material

Figure 4 gave the result of the average temperature of the drying material in the drying process. Figure 4 showed that in RF-assisted HP drying, the heating rate was significantly more than HP-only drying. This was indicated by the fact that when RF power increased, more RF energy was absorbed within the material. Thus, the wet dipole molecules and free ions in the material would oscillate faster, which caused the heat generation inside the material to become faster and increased the heating rate [20], [21]. In the RF-assisted HP drying process, after the material's temperature reached the drying air temperature, the temperature of the material increased beyond the drying air temperature. The moisture within the material continued to absorb the RF energy, making the material's temperature continue to increase. This result was agreed with the previous studies of the RF heating mechanism [9], [22]. However, after the material temperature reached the highest value, it decreased to the drying air temperature value. This stage extended to the end of the drying process. The reasons for this were: (i) the decrease of moisture content of drying material causes the RF energy absorption within the material to decrease; (ii) the heat absorbed during this stage is used only to maintain the vaporization of moisture the material. This result was agreed with the study of the RF heating mechanism given by Samet Ozturk et al. [23].

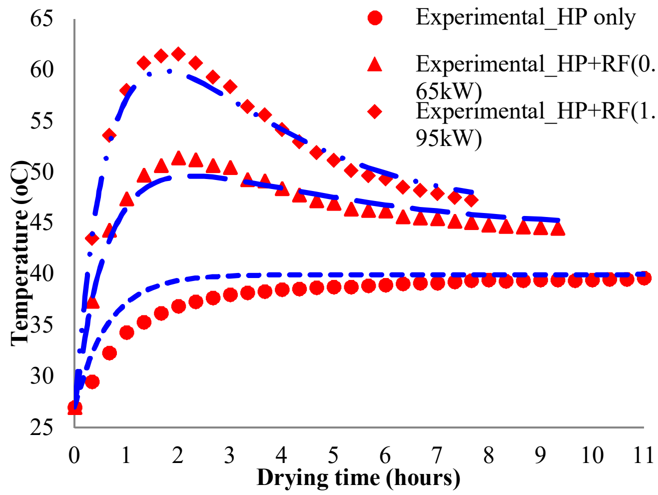

Fig. 4 Average temperature of drying material versus drying time

Figure 5 gave the experimental results of the temperature value at the center and surface of the drying material. Figure 5 showed that in RF-assisted HP drying, the center's temperature value was lower than on the material's surface at the first stage of the drying process. It could be explained that the surface of the material absorbed the heat by RF heating and heat convection mechanism while the center of material only absorbed the heat by RF heating mechanism.

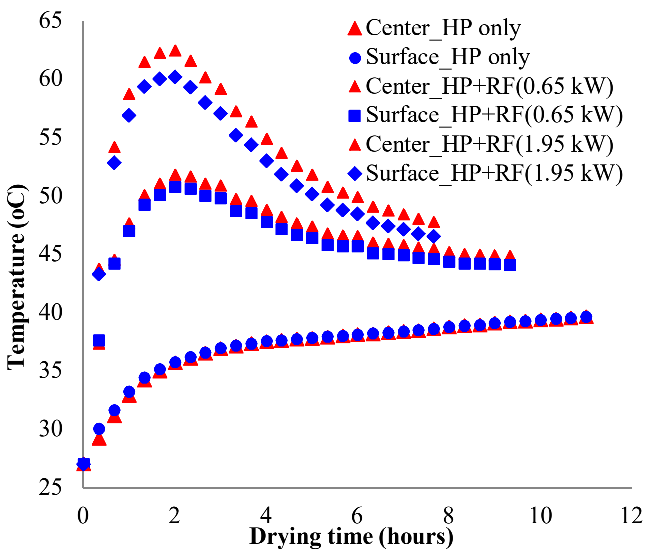

Fig. 5 Temperature at center and surface of drying material versus drying time.

This stage lasted 30 minutes and 20 minutes, corresponding to output RF power of 0.65 and 1.95 kW. At the next stage that lasted to the end of the drying process, the center's temperature value was higher than at the surface of material because of the volumetric RF heating mechanism. Thus, the temperature gradient had the same direction as the moisture gradient, making the moisture diffusion process within the drying material occur faster. It could be explained that the moisture content at the center was higher and absorbed more RF energy than at the surface of the material, and this is the advantage of the RF heating mechanism in drying technology. In HP only drying, the center's temperature value was always lower than the material's surface during the drying process because of the convective heat exchange mechanism. Thus, the temperature gradient and the moisture gradient were opposite, affecting the moisture diffusion process within the drying material.

B. Effect of Output RF Power on the Moisture Content of Drying Material

Figure 6 showed the average moisture content of the material in the drying process.

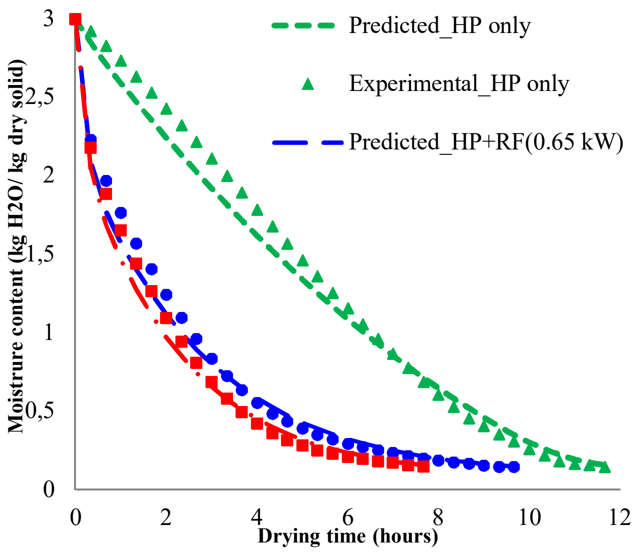

Fig. 6 Average moisture content of drying material versus drying time.

Fig. 6 showed that the RF-assisted HP drying method improved the drying rate and the drying time was shortened significantly as comparing to HP only drying. The reason for this was the fact that when RF power increased, the heating rate increased. Thus, the vaporization and moisture diffusion within the material during the drying process occurred faster. This result was similar to previous studies of RF heating mechanism for agricultural products [24], [25]. The drying time was 465, 555 and 700 minutes corresponding to output RF power of 1,.95 kW, 0.65 and 0 kW. At output RF power of 1.95 kW, the drying time decreased 16% and 34% comparing with drying time at an output RF power of 0.65 kW and 0 kW.

C. Evaluating the Mathematical Drying Model

The difference between the mathematical heat and mass equations solving results (predicted data) and experimental drying data (experimental data) presented in Fig. 4 and Fig. 6 can be attributed to several factors. Firstly, in experimental drying, the moisture diffusion coefficient varies slightly as the dried product undergoes warpage, and the shrinkage occurs. However, in the present mathematical model, deformations of material are small and negligible. Secondly, the assumption in the present model of full heat transfer symmetry between upper and lower surfaces of material is not strictly valid due to the mesh grid is partially masking the lower surface.

To evaluate the difference between predicted data and experimental data, a two-sample comparison analysis was conducted by Statgraphics Centurion XVII on the computer to identify the value of P-Ratio and the values of RMSE, MAE is calculated by Eq. (14) and Eq. (15). The result was given in Table 2.

Table 2 showed that the P-value was higher than 0.05, so there was not a statistically significant difference between the predicted data and experimental data at the confidence level of 95%. Besides, the value of RMSE and MAE was relatively low. Thus, the analyzing results confirmed that the proposed mathematical model accurately reproduced the experimental data reported

TABLE II
THE ANALYZING PARAMETERS OF COMPARING THE MATHEMATICAL HEAT AND MASS EQUATIONS SOLVING RESULTS AND EXPERIMENTAL DRYING DATA

Drying mode	**The moisture content value**		
	P-Value	RMSE	MAE
HP only drying	0.77	0.03	4.6%
HP+RF (0.65 kW)	0.88	0.03	6.6%
HP+RF (1.95 kW)	0.86	0.05	6.4%
Drying mode	**The temperature value**		
	P-Value	RMSE	MAE
HP only drying	0.07	1.1	2.2%
HP+RF (0.65 kW)	0.98	0.79	1.3%
HP+RF (1.95 kW)	0.94	0.94	1.5%

IV. CONCLUSION

This study proposed a mathematical model that could be used to predict the temperature and moisture content of the drying material during RF assisted HP drying process. The finite difference method methodology was established to solve the simultaneous heat and mass transfer equations by *pdepe* function on Matlab software. The predicted data and experimental data showed that the RF power increase increased the heating rate and drying rate significantly. A considerably good agreement between the predicted data and experimental data was found for its temperature and moisture.

NOMENCLATURE

C_p	specific heat capacity	J/kg.°C
M_e	equilibrium moisture content	d.b
M_i	initial moisture content	d.b
t	temperature	°C
T	absolute temperature	K
R_H	drying air humidity	%
M	moisture content	d.b
r	latent heat of vaporization of moisture	J/kg

Greek letters

δ	thickness	m
λ	thermal conductivity	W/m.°C
ρ	density	kg/m^3
α	convective heat transfer coefficient	W/m^2.°C
β_M	convective mass transfer coefficient	m/s
V_{Exp}	experimental value of moisture content or temperature	
V_{Pre}	predicted value of moisture content or temperature	

Subscripts

a	drying air
e	equilibrium

i initial

s surface

REFERENCES

[1] Perumal K., *Indigenous technology on organic cultivation of Reishi (Ganoderma lucidum)*, Taramani, Chennai 600 113, Chennai: Shri AMM Murugappa Chettiar Research Centre, 2009.

[2] Chin S.K., Law C.L., Supramaniam C.V., Cheng P.G., "Thin layer drying characteristics and quality evaluation of air-dried Ganoderma Tsugae Murill", *Journal Drying Technology*, Vol. 27, pp. 975–984, 2009.

[3] Siew Kian Chin, Chung Lim Law, Poh Guat Cheng, "Effect of drying on crude Ganoderic acids and water soluble Polysaccharides content in Ganoderma lucidum", *International Journal of Pharm Science,* Vol. 3, No.1, pp. 38–43, 2011.

[4] Prasetyo D.J., Jatmiko T.H., Poeloengasih C.D., Kismurtono M., *Drying characteristics and water-soluble polysaccharides evaluation of kidney shape Ganoderma lucidum drying in air circulation system*, IOP Conf. Series: Earth and Environmental Science 101 (2017) 012012, 2017.

[5] Nguyen Hay, Le Anh Duc, Pham Van Kien, "Study on designing and manufacturing a Radio frequency generator using in drying technology", *IEEE Xplore Digital library*, ISBN: 978-1-5386-5125-4, DOI: 10.1109/GTSD. 2018.8595618, pp. 416–422, 2018.

[6] Jumah R., "Modelling and simulation of continuous and intermittent Radio Frequency-Assisted fluidised bed drying of grains", *Journal of Food Bioprod Process*, Vol. 83, pp. 203–210, 2005.

[7] Ptasznik W., Zygmunt S., Kudra T., "Simulation of RF-Assisted convective drying of seed quality broad Beans", *International Journal of Drying Technology*, Vol. 8, pp 977–992, 1990.

[8] Marshall M.G., Metaxas A.C., "A Novel Radio Frequency Assisted Heat Pump Dryer", *International Journal of Dry Technology*, Vol. 17, pp. 1571–1578, 1999.

[9] Zhi Huang, BoZhang, Francesco Marra, ShaojinWang, "Computational modelling of the impact of polystyrene containers on radio frequency heating uniformity improvement for dried soybeans", *Journal of Innovative Food Science and Emerging Technologies*, Vol. 33, pp. 365–380, 2016. .

[10] Zhi Huang, Francesco Marra, Shaojin Wang, "A novel strategy for improving radio frequency heating uniformity of dry food products using computational modeling", *Journal of Innovative Food Science and Emerging Technologies*, Vol. 34, pp. 100–111, 2016.

[11] Ferruh Erdogdu, Ozan Altin, Francesco Marra, Tesfaye Faye Bedane, "A computational study to design process conditions in industrial radio-frequency tempering/thawing process", *Journal of Food Engineering,* Vol. 213, pp. 99–112, 2017.

[12] Hankun Zhu, Dong Li, Shujun Li, Shaojin Wang, "A novel method to improve heating uniformity in mid-high moisture potato starch with Radio frequency assisted treatment", *Journal of Food Engineering*, Vol. 206, pp. 23–36, 2017.

[13] Rahmi Uyara, Ferruh Erdogdub, Fabrizio Sarghini, Francesco Marrad, "Computer simulation of radio-frequency heating applied to block-shaped foods: Analysis on the role of geometrical parameters", *Journal of Food and Bio products Processing*, Vol. 9, No. 8, pp. 310–319, 2016.

[14] Samet Ozturk, Fanbin Kong, Samir Trabelsi, Rakesh K. Singh, "Dielectric properties of dried vegetable powders and their temperature profile during radio frequency heating", *Journal of Food Engineering*, Vol. 169, pp. 92 - 100, 2016.

[15] Xuan Quang Nguyen, Anh Duc Le, Ngoc Phuong Nguyen, Hay Nguyen, " Thermal diffusivity, moisture diffusivity, and color change of Codonopsis Javanica with the support of the ultrasound for drying", *Journal of Food Quality*, Vol. 2019, Article ID 2623404, 13 pages, 2019.

[16] Le Anh Duc, "Study on circulating conccurrent flow dryer for drying Papessed", *International Journal on Advanced Science, Engineering and Information Technology*, Vol. 5, pp. 367–371, 2015.

[17] Han J.W., Keum D.H., Kim W., Duc L.A., Cho S.H., Kim H., "Circulating concurrent-flow drying simulation of rapeseed", *Journal of Biosystems engineering*, Vol. 35(6), 401–407, 2010.

[18] Pham Van Kien, Le Anh Duc, Nguyen Hay, "Research of thermo - physical properties of Ganoderma lucidum", *Journal of thermal energy,* Vol. 142, pp. 11–15, 2018.

[19] Pham Van Kien, Nguyen Hay, Le Anh Duc, "Equilibrium Moisture Content of Ganoderma Lucidum", *Journal of Applied Mechanics and Materials,* ISSN: 1662-7482, Vol. 889, pp. 266–274, 2019.

[20] Lixia Houa, Bo Linga, Shaojin Wang, "Development of thermal treatment protocol for disinfesting chestnuts using Radio frequency energy", *Journal of Postharvest Biology and Technology*, Vol. 98, pp. 65–71, 2016.

[21] Samet Ozturk, Fanbin Kong, Rakesh K. Singh, Jese Daniel Kuzy và Changying Li, "Radio frequency heating of corn flour: Heating rate and uniform", *Journal of Innovative Food Science and Engineering technology*, Vol. 171, pp. 234–241, 2017.

[22] Wang, S., Tang, J., Johnson, J.A., Cavalieri, R.P., "Heating uniformity and differential heating of insects in almonds associated with radio frequency energy", *Journal of Stored Prod. Res*, Vol. 55, pp. 15–20, 2013.

[23] Samet Ozturka, Fanbin Kong, Samir Trabelsi và Rakesh K. Singh, "Dielectric properties of dried vegetable powders and their temperature profile during Radio frequency heating", *Journal of Food Engineering,* Vol. 169, pp. 91–100, 2016.

[24] Darvishi H, Asl AR, Asghari A, Najafi G, Gazori HA, "Mathematical Modeling, Moisture Diffusion, Energy consumption and Efficiency of Thin Layer Drying of Potato Slices", *Journal of Food Process Technology*, Vol. 4, No. 3, pp. 234–241, 2013.

[25] Ahmet Kaya, "Numerical Analysis Of A Radio Frequency Assisted Convective Drying", *International Journal of Scientific and Technology Research,* Vol. 4, No. 6, pp. 234–241, 2015.